Extension of the isobar model for intranuclear cascades to 1 GeV†

G. D. Harp*
Chemistry Department, Brookhaven National Laboratory, Upton, New York 11973
(Received 16 September 1974)

An intranuclear cascade model is proposed for studying pion and nucleon induced reactions in the region of single pion production. The model explicitly considers the production and subsequent interactions of (3,3) isobars. The predictions of the model are compared with experimental data from proton induced reactions such as pion production yields, pion and proton energy and angular distributions, and spallation yields. The model gives a fair to excellent representation of all these data.

I. INTRODUCTION

In a previous paper[1] (hereafter referred to as I), an intranuclear cascade model was proposed for studying low-energy pion induced nuclear reactions. In contrast to previous intranuclear cascade models,[2-5] this model assumed that in elastic pion-nucleon collisions, within the nucleus (3, 3) isobars were formed. Once formed, these isobars could then decay or they could interact with other nucleons. Two types of isobar-nucleon interactions were discussed: isobar capture and isobar-nucleon "exchange" scattering (see I for further details). A comprehensive comparison of the predictions of the model with experiment was not made because of the scarcity of experimental information on low-energy pion-nucleus interactions. However, those comparisons that were made indicated that the predictions of the model were in reasonable agreement with experiment.

This model has recently been extended such that it now includes the production and subsequent interactions of inelastically produced isobars as well; that is, isobars produced in inelastic nucleon-nucleon and pion-nucleon interactions. At present, this model only considers single isobar or pion production in inelastic collisions. Hence, it is only applicable for bombarding energies less than approximately 1 GeV.

In the next section some of the details of the model will be given. In subsequent sections the predictions of the model will be compared with various experimental data from proton induced reactions such as pion production yields, pion and secondary nucleon spectra, and radiochemical yields. The model gives a fair to excellent representation of all these data.

II. DETAILS OF MODEL

The present model assumes that inelastic isobars undergo the same interactions within a cascade as those produced in elastic pion-nucleon interactions. That is, they can capture, "exchange" scatter, or decay. A detailed description of each of these interaction mechanisms, as well as other relevant information concerning the model are given in I. Therefore, in the following, only the elementary cross sections and isobar production mechanisms that were used will be discussed.

A. Elementary interaction cross sections

The total cross sections for nucleon-nucleon collisions[6,7] above 400 MeV that were used are shown in Fig. 1. Below 400 MeV the total cross sections given in Ref. 8 were used.

The cross sections for single pion or isobar production in p-p collisions were taken to be the sum of the cross sections for the reactions $p+p \rightarrow 2p+\pi^0$ and $p+p \rightarrow n+p+\pi^+$ that are illustrated in Fig. 2.[3,9] For p-n collisions the single pion or isobar cross sections were taken to be $\sigma(p+n \rightarrow p+n+\pi^0)+2\sigma(p+n \rightarrow 2p+\pi^-)$. These latter partial cross sections are illustrated in Fig. 2.[10-14] The cross sections for $p+n \rightarrow 2p+\pi^-$ above 1.5 GeV were obtained by a linear fit between the experimental points near 1 GeV and the single experimental point of Shapira *et al.* at 7 GeV/c.[12] The cross sections for $p+n \rightarrow \pi^0+p+n$ above 1 GeV were obtained with the aid of the relation $\sigma(p+n \rightarrow \pi^0+p+n) = \frac{1}{2}\sigma(p+p \rightarrow n+p+\pi^+)+\sigma(p+n \rightarrow 2p+\pi^-) - \sigma(p+p \rightarrow 2p+\pi^0)$ which follows from isotopic spin considerations.

The elastic nucleon-nucleon cross section was taken to be the difference between the total cross section and the cross section for producing one pion. Hence, the elastic cross sections are only valid below about 1 GeV. The angular distributions that were used in elastic nucleon-nucleon collisions were those given in Ref. 15.

Below 320 MeV, pion-nucleon interactions were again assumed to form $T=\frac{3}{2}$ isobars. Above 320 MeV, elastic isobar formation in pion-nucleon in-

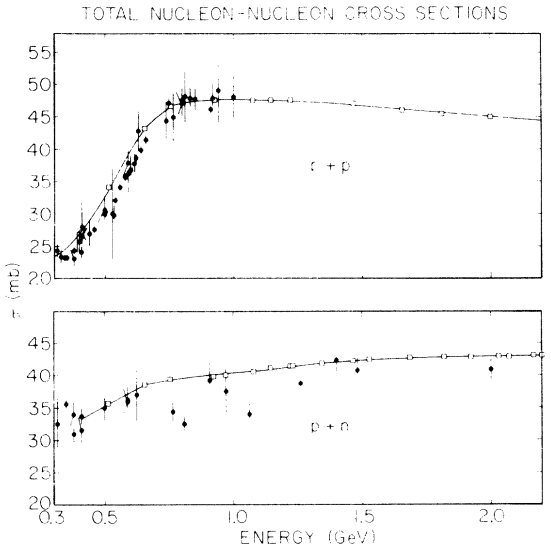

FIG. 1. Total proton-proton and proton-neutron cross sections. The points are the experimental data contained in the compilation of Barashenkov and Maltsev (Ref. 6). The open squares are the experimental data of Bugg *et al.* (Ref. 7).

teractions was assumed to no longer occur. That is, above this energy neither pion-nucleon elastic nor charge exchange scattering was assumed to proceed through an isobar intermediate. This energy was chosen as the cutoff for elastic isobar formation since at higher energies pion production in pion-nucleon interactions begins to occur. In addition, at higher energies one can no longer assume that the $T=\frac{1}{2}$ contribution to pion-nucleon interactions is negligible.

The total and elastic π^+-p and the total, elastic, and charge exchange π^--p cross sections were taken from the compilation of Giacomelli *et al.*[16] The cross section for single pion production in π^+-p collisions was taken to be the difference between the total and elastic cross sections. Similarly, for π^--p collisions the single pion production cross section was taken to be the difference between the total and the sum of the elastic and charge exchange cross sections. The total cross section and the cross section for producing one pion in π^0-n and π^0-p collisions were taken to be the arithmetic means of the corresponding cross sections for π^+-p and π^--p collisions. The elastic π^0-n and π^0-p cross sections were evaluated in the same manner used previously.[1] The angular distributions for π^+-p and for π^--p elastic scattering, as well as for π^--p charge exchange scattering, were obtained as before from parabolic fits to the experimental data contained in the compilation of Giacomelli *et al.*[16]

B. Inelastic isobar production

Three models for isobar production in inelastic nucleon-nucleon collisions were investigated: the Sternheimer-Lindenbaum (SL) model,[17] the peripheral or one-pion-exchange (OPE) model in the pole approximation,[18] and the OPE model approximately modified to include the phenomonological pion-nucleon form factor of Suslenko and Kochkin.[19] Assuming isobar formation to proceed only through the $T=\frac{3}{2}$ state and assuming incoherence between the contributions to a given final state, the partial cross sections for isobar production are given by:

$$\sigma(p+p\to\Delta^{++}+n)=\tfrac{3}{4}\sigma_{1\pi}^{pp}\ ,$$

$$\sigma(p+p\to\Delta^{+}+p)=\tfrac{1}{4}\sigma_{1\pi}^{pp}\ ,$$

$$\sigma(p+n\to\Delta^{+}+n)=\tfrac{1}{2}\sigma_{1\pi}^{pn}\ ,$$

$$\sigma(p+n\to\Delta+p)=\tfrac{1}{2}\sigma_{1\pi}^{pn}\ ,$$

where Δ is a (3, 3) isobar, and $\sigma_{1\pi}^{pp}$ and $\sigma_{1\pi}^{pn}$ are the cross sections for producing one pion in p-p and p-n collisions, respectively. The cross sections for Δ formation in n-n collisions are related to those for p-p collisions by charge independence.

In the Sternheimer-Lindenbaum model[17] the isobar mass distribution is given by

$$P(V,U)=A\sigma_{33}(V)F(V,U)\ ,$$

where V is the mass of the isobar, U is the total center of mass (c.m.) energy of the initial nucleon-nucleon system, $\sigma_{33}(V)$ is the π^+-p cross section evaluated at a total pion-nucleon c.m. energy V, F is a two body phase factor for the produced nucleon and isobar, and A is a normalization factor. The isobar angular distribution in the c.m. of the original nucleon-nucleon system was assumed to be $\frac{3}{4}\cos^2\theta+\frac{1}{4}$ where θ is the angle of production.

The isobar mass and angular distribution for the OPE model in the pole approximation[18] is given by

$$P(V,U,\cos\theta)=B\sigma_{33}(V)p_v V^2\frac{t^2}{(t^2+\mu^2)^2}\ ,$$

where B is a normalization factor, μ is the pion mass, p_v is the internal momentum of the isobar (i.e., the momentum of either the decay pion or nucleon in the c.m. of the isobar, once the isobar decays), and t^2 is the invariant square of the four-momentum of the exchanged pion (see Ref. 18 for further details).

The isobar mass and angular distribution for the modified OPE model was obtained simply by multiplying the pole approximation distribution by[19]

$$G^2(t^2)=\left[\frac{9\mu^2}{10\mu^2+t^2}\right]^2\ .$$

The factor G^2 is one of the modifications to the pole approximation that must be made to correct for the virtuality of the exchange pion. The other modifications associated with the scattering of the virtual pion from a nucleon were not made.[18,19]

In Fig. 3 the experimental[20] p, n, and π^+ energy distributions for the $p+p \rightarrow \pi^+ + p + n$ reaction at 970 MeV are compared with the predictions of all three models. In all calculations it was assumed that the isobar underwent p-wave decay after production. All of the models represent the experimental π^+ distribution quite well. However, the calculated nucleon distributions differ from each other as well as from experiment. The modified OPE model represents the experimental data the best. However, the Sternheimer-Lindenbaum model also gives an adequate representation of the data. The pole approximation is clearly inferior to the other two models in reproducing the experimental nucleon distributions.

In Fig. 4 calculated and experimental[21] π^+ energy distributions from inelastic p-p interactions

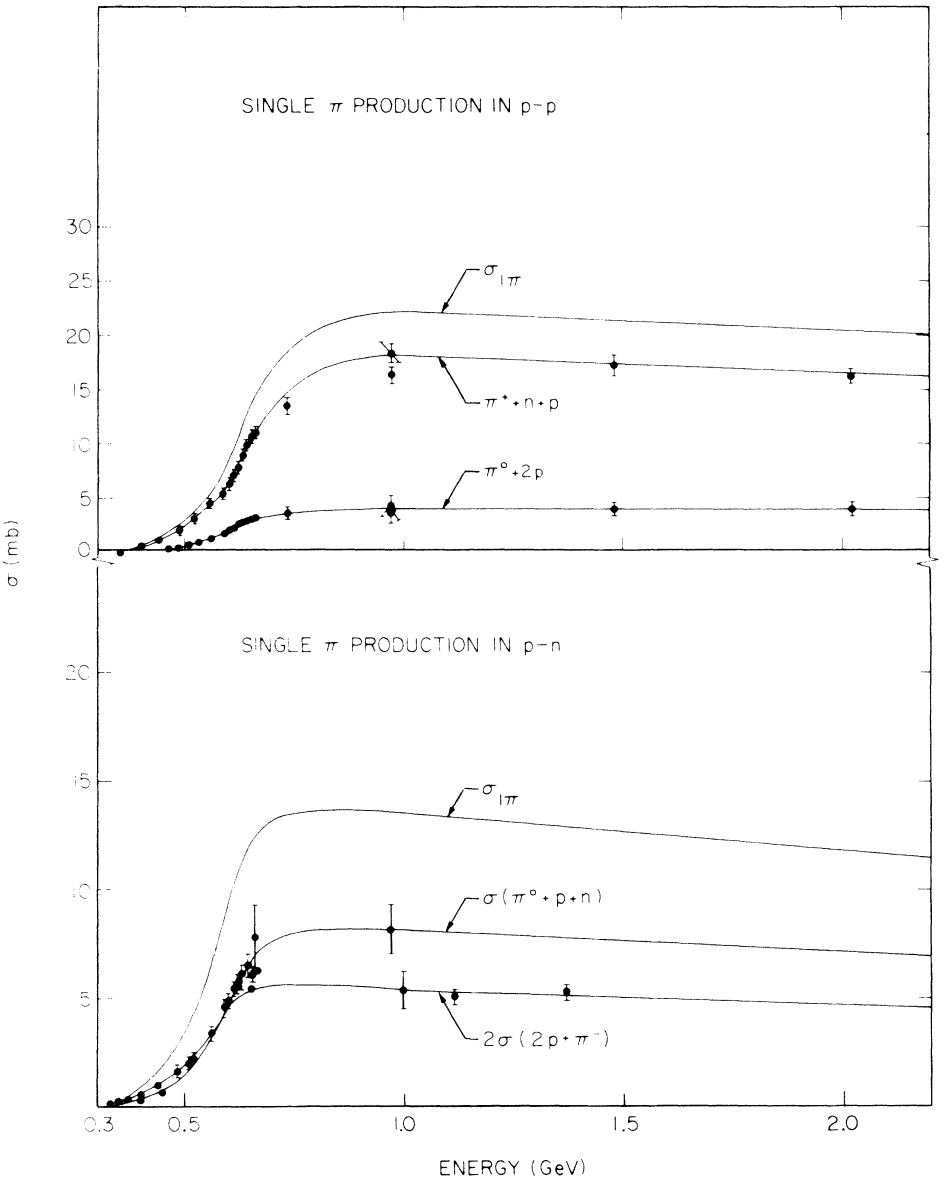

FIG. 2. Single pion production cross sections in nucleon-nucleon collisions. The partial cross sections $\sigma(pp \rightarrow \pi^0 + 2p)$ and $\sigma(pp \rightarrow \pi^+ + n + p)$ were taken from Refs. 3 and 9. The cross sections for $pn \rightarrow 2p + \pi^-$ were taken from Refs. 10, 11, and 12. The cross sections for $pn \rightarrow \pi^0 + p + n$ were taken from Refs. 10, 13, and 14.

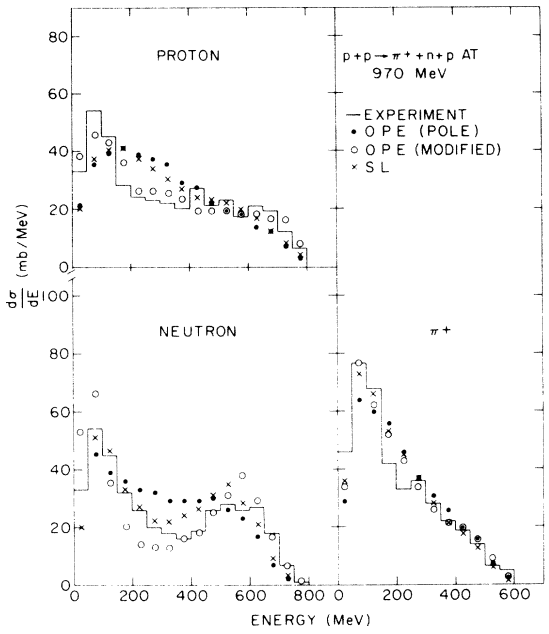

FIG. 3. Calculated and experimental (Ref. 20) pion and nucleon spectra for the reaction $pp \rightarrow \pi^+ + n + p$ at 970 MeV. In all calculations it was assumed that the inelastic isobar underwent p-wave decay. SL refers to the Sternheimer-Lindenbaum model.

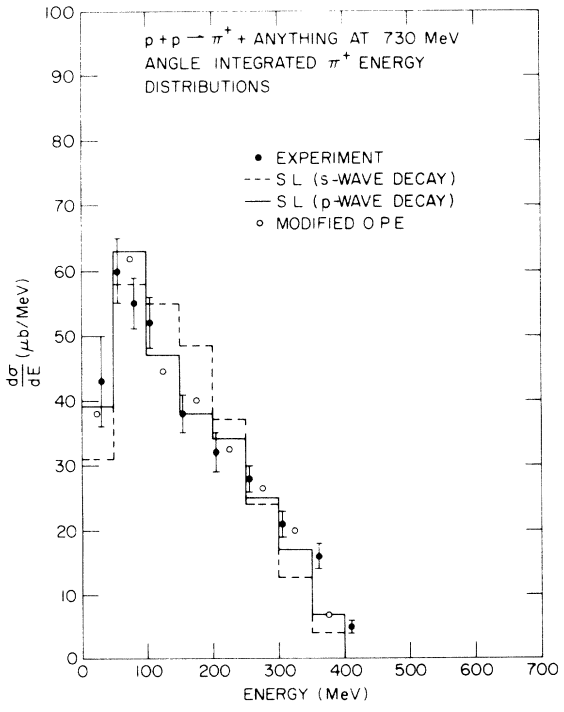

FIG. 4. Calculated and experimental (Ref. 21) π^+ energy distributions from inelastic p-p interactions at 730 MeV.

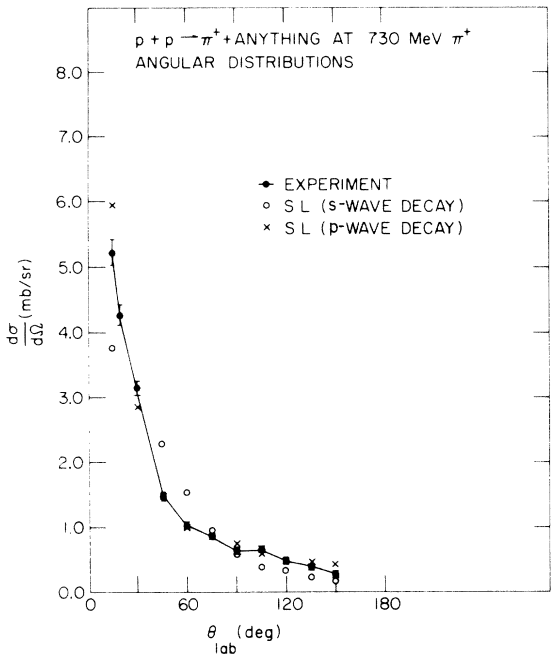

FIG. 5. Calculated and experimental (Ref. 21) π^+ angular distributions from inelastic p-p interactions at 730 MeV.

at 730 MeV are presented. The effects of p-wave versus s-wave decay of the isobar after production are illustrated by the two Sternheimer-Lindenbaum distributions. The p-wave decay distribution is clearly in better agreement with experiment. The modified OPE distribution which is shown in this figure and the pole approximation distribution which is not shown were both obtained assuming p-wave isobar decay. Both distributions are almost indistinguishable from the Sternheimer-Lindenbaum distribution which assumes the same isobar decay angular distribution.

In Fig. 5 the experimental π^+ angular distribution[21] for inelastic p-p interactions at 730 MeV are compared with two Sternheimer-Lindenbaum distributions: one for p-wave and the other for s-wave isobar decay. The distribution based on p-wave decay is clearly in better agreement with experiment. Both the modified OPE and pole approximation distributions (not shown) which assumed p-wave decay are almost indistinguishable from the corresponding Sternheimer-Lindenbaum distribution. Hence, all three models yield comparable π^+ energy and angular distributions provided the same isobar decay angular distributions are used. Further, the experimental data are best represented by p-wave decay. Since the Sternheimer-Lindenbaum model with p-wave isobar decay gives a reasonable description of the

TABLE I. Calculated and experimental (data of Cochran *et al.*, Ref. 21) π^+ and π^- production cross sections for the interaction of 730-MeV protons with various nuclei. All cross sections are in mb.

Nucleus	Exp.	ISONEX-NO	ISONEX
	$\sigma(\pi^+)$		
Pb	104.2 ± 5.8	98.6 ± 3.4	88.0 ± 3.3
Cu	77.3 ± 4.3	76.8 ± 2.7	70.9 ± 2.3
Al	53.1 ± 2.9	62.3 ± 1.8	
C	35.0 ± 1.8	43.8 ± 1.3	
	$\sigma(\pi^-)$		
Pb	53.7 ± 4.9	49.5 ± 2.4	48.0 ± 2.4
Cu	25.2 ± 2.0	27.1 ± 1.6	27.7 ± 1.4
Al	13.2 ± 0.9	17.4 ± 0.9	
C	6.6 ± 0.4	9.2 ± 0.6	
	$\sigma(\pi^+)/\sigma(\pi^-)$		
Pb	1.95 ± 0.2	2.0 ± 0.1	1.8 ± 0.1
Cu	3.1 ± 0.3	2.8 ± 0.2	2.6 ± 0.2
Al	4.0 ± 0.3	3.6 ± 0.2	
C	5.3 ± 0.4	4.8 ± 0.3	

experimental data and uses less computer time than the other two models, it was used in the intranuclear cascade model for inelastic isobar production in nucleon-nucleon collisions.

The Sternheimer-Lindenbaum model was also used for inelastic isobar production in pion-nucleon collisions. The isobar angular distribution in the c.m. of the original pion-nucleon system was again taken to be $\frac{3}{4}\cos^2\theta + \frac{1}{4}$. The inelastic isobar was forced to undergo p-wave decay.

Two additional quantities, ρ and a, are needed by the isobar model[17] to completely specify the distribution of final state products. ρ and a are defined by

$$\rho = \frac{\sigma_{3/2}(1\pi)}{2\sigma_{1/2}(1\pi)}\,, \quad a = \sqrt{\rho/5}\,\cos\phi\,,$$

where $\sigma_{3/2}(1\pi)$ and $\sigma_{1/2}(1\pi)$ are the single pion production cross sections in the $T=\frac{3}{2}$ and $T=\frac{1}{2}$ states, respectively. ϕ is the phase angle between the matrix elements for pion production in the $T=\frac{1}{2}$ and $\frac{3}{2}$ states.

ρ and a were evaluated from the following relations:

$$\frac{\sigma(\pi^- + p \to \pi^- + p + \pi^0)}{\sigma(\pi^- + p \to \pi^+ + \pi^- + n)} = \frac{(10 + 17\rho - 25a)}{(25 + 26\rho + 35a)}\,,$$

$$\frac{\sigma(\pi^- + p \to 2\pi^0 + n)}{\sigma(\pi^- + p \to \pi^+ + \pi^- + n)} = \frac{(10 + 2\rho - 10a)}{(25 + 26\rho + 35a)}\,.$$

The values of ρ and a which were obtained using the experimental cross sections compiled by Barashenkov *et al.*[9] between 500 and 800 MeV were 0.0791 and −0.124, respectively. These values were then used for all energies.

TABLE II. Calculated and experimental (data of Dunaitsev *et al.*, Ref. 22) π^0 production cross sections for the interaction of 660-MeV protons with various nuclei. All cross sections are in mb.

Target	$\sigma(\pi^0)$ Exp.	ISONEX-NO	Bertini [a]
Pb	143 ± 8.0	89.5 ± 6.6	200 ± 12
Cu	73.4 ± 4.2	58.4 ± 3.2	109 ± 12
Al	45.9 ± 2.6	41.2 ± 2.9	60 ± 4
C	27.3 ± 1.5	30.2 ± 1.5	35

[a] The calculated values of Bertini (Ref. 3).

III. COMPARISON TO EXPERIMENT

A. Pion production

The emission of pions is one characteristic of high-energy nuclear reactions that provides a severe test of the pion production and pion absorption mechanisms assumed in the present model. In Table I calculated and experimental[2] cross sections for the production of both positive and negative pions from the interaction of 730-MeV protons

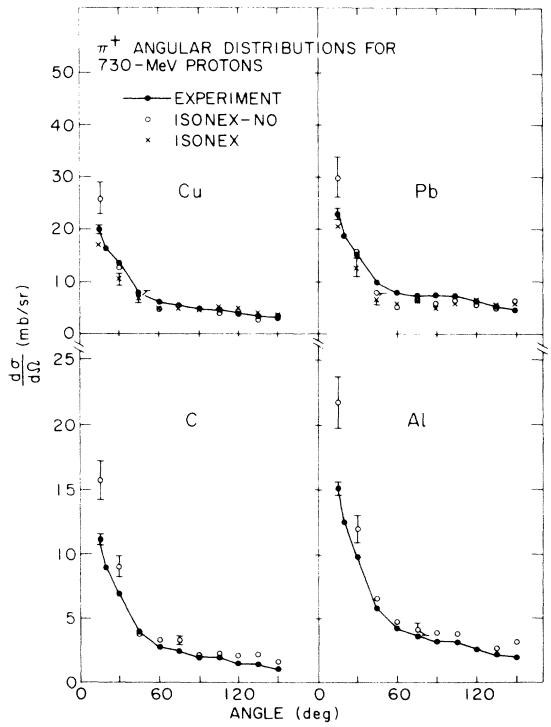

FIG. 6. Calculated and experimental (Ref. 21) π^+ angular distributions from the interaction of 730-MeV protons with C, Al, Cu, and Pb.

with various targets are presented. Two sets of calculated results are given for Cu and Pb. In one (ISONEX) isobar-nucleon "exchange" scattering was included while in the other (ISONEX-NO) this interaction was neglected. For the two heavier elements (Cu and Pb) the ISONEX-NO cross sections for both positive and negative pions agree quite well with experiment. For Al and C the ISONEX-NO results are somewhat high. "Exchange" scattering has little or no effect on negative pion emission while it slightly suppresses the emission of positive pions. The experimental π^+/π^- ratios are also well represented by the ISONEX-NO model while the ISONEX ratios are somewhat too low. If the inelastic isobars were formed and then escaped without further interaction, the ratios would be a great deal larger (e.g., in the case of C the ratio would be $\frac{11}{1}$ instead of the calculated and experimental value of $\sim\frac{5}{1}$). The increased π^- emission has been attributed to the pion-nucleon charge exchange reaction $\pi^0 + n \rightarrow \pi^- + p$.[21]

In Table II calculated and experimental[22] π^0 production cross sections for the interaction of 660-MeV protons with various targets are given. The calculated values for the two lightest targets (C and Al) agree fairly well with experiment. However, for the heavier targets (Cu and Pb) the model underestimates the number of emitted π^0. Bertini[3] has also compared the results of his calculation with this set of experimental data. In each case his predicted cross sections, which are also given in Table II, are higher than experiment.

Figure 6 presents calculated and experimental[21]

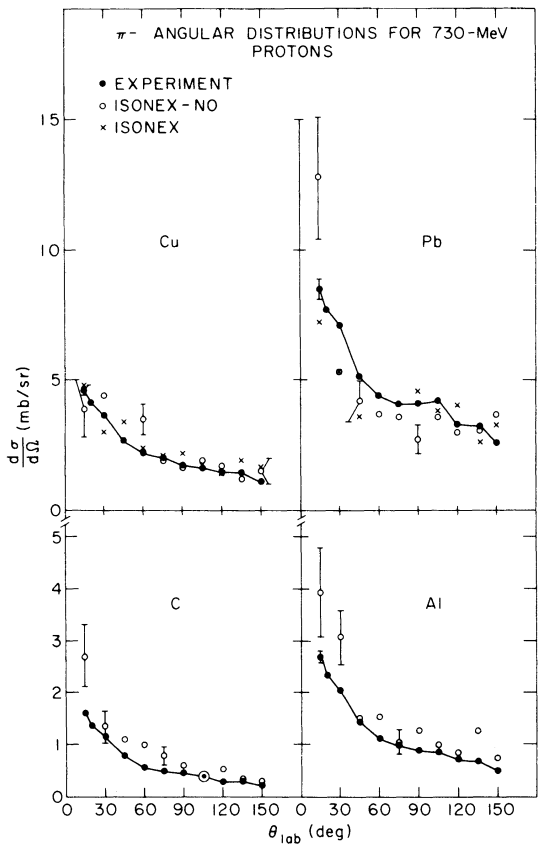

FIG. 7. Same as Fig. 6 but for π^- production.

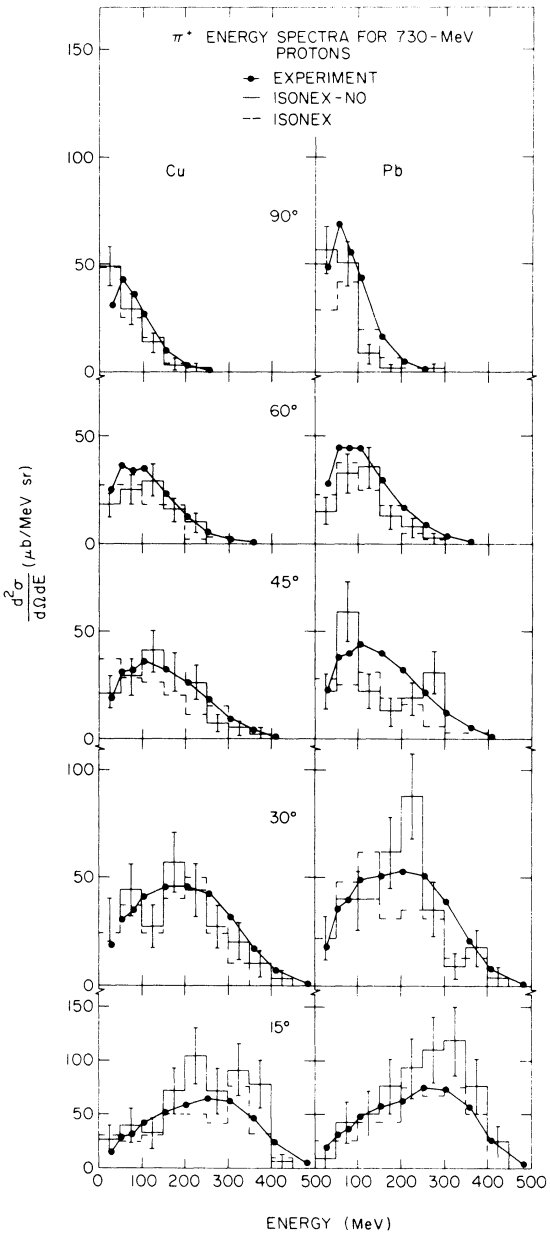

FIG. 8. Calculated and experimental (Ref. 21) π^+ energy spectra from the interaction of 730-MeV protons with Cu and Pb. The spectra are given at 15°, 30°, 45°, 60°, and 90°.

π^+ angular distributions from the interaction of 730-MeV protons with various targets. The ISONEX-NO results for Cu and Pb show good agreement with experiment except perhaps at 15° where the calculated results are somewhat too high. However, the introduction of exchange scattering removes this slight discrepancy. On the other hand, the calculated distributions for C and Al are uniformly too high. This is partially due to the fact that the calculated π^+ yields for these two targets were larger than experiment (see Table I).

Calculated and experimental[21] π^- angular distributions are compared in Fig. 7. The calculated distributions for Cu and Pb again agree fairly well with experiment while the calculated distributions for C and Al are again uniformly too high.

Calculated and experimental[21] π^+ energy spectra from Cu and Pb at various angles are presented in Fig. 8. Both the shapes and magnitudes of the experimental spectra are fairly well represented by the calculation. The introduction of exchange scattering leads to a slight shift in the calculated spectra toward lower energies.

Calculated and experimental[21] π^- spectra for Cu and Pb are compared in Fig. 9. In this case the introduction of exchange scattering leads to slightly better agreement with experiment. However,

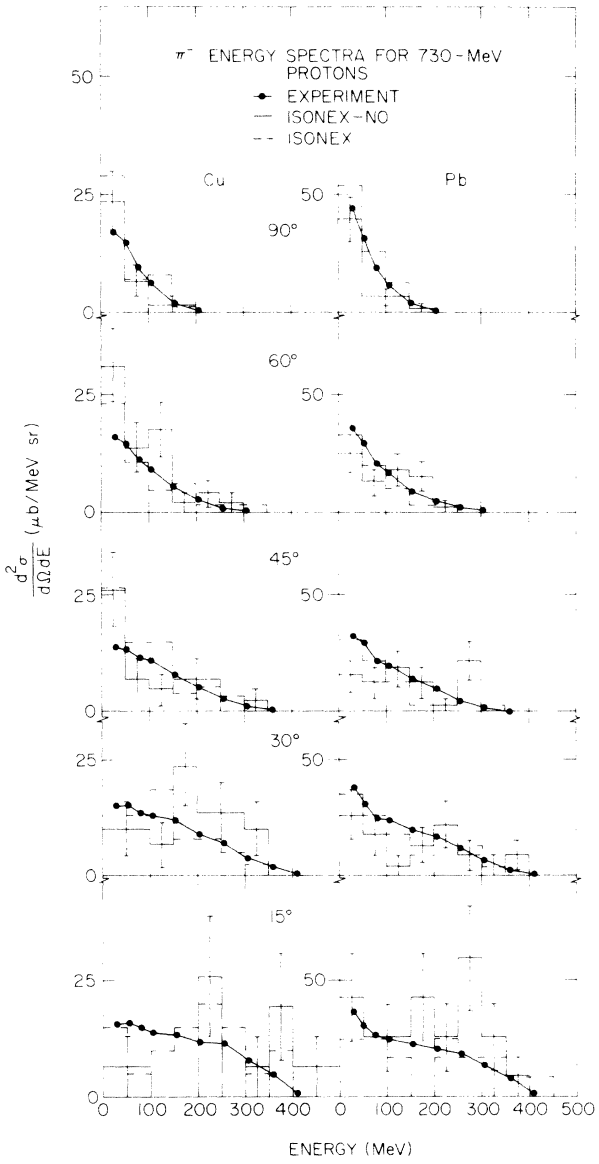

FIG. 9. Same as Fig. 8 but for π^-.

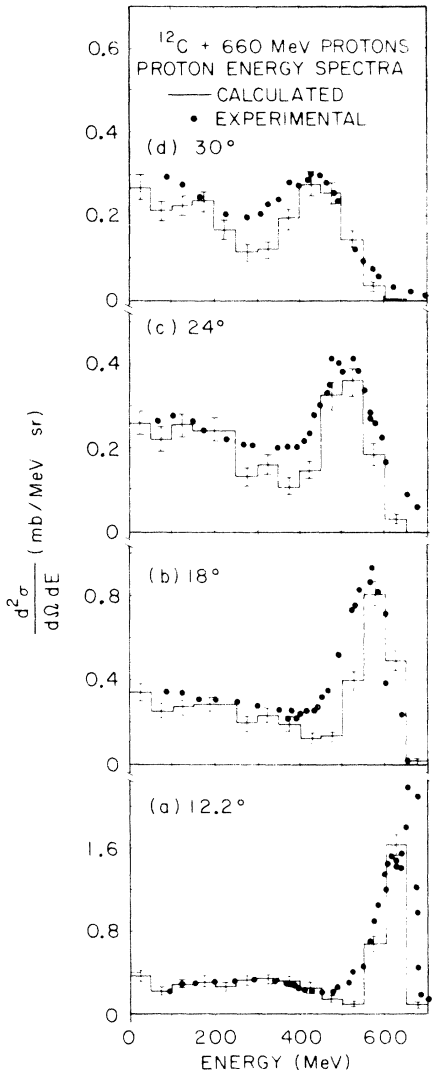

FIG. 10. Energy spectra of inelastic protons from the interaction of 660-MeV protons with C. The spectra are given at 12.2°, 18°, 24°, and 30°. The experimental points are taken from Ref. 23.

neither calculation represents the experimental data at 15° very well.

B. Energy spectra of emitted protons

Another characteristic of high-energy nuclear reactions that provides a direct test of the cascade model is the emission of high-energy nucleons. In Figs. 10 and 11 calculated and experimental[23] proton energy spectra at various angles from the interaction of 660-MeV protons with C and Cu are compared. The positions and magnitudes of the experimental quasifree scattering peaks as well as the distributions of low-energy protons arising from multiple scattering and pion production events are well represented by the calculation. Bertini[3] has also compared the predictions of his model with these experimental results and finds a similar degree of agreement.

Further comparisons between calculated and experimental[24] proton spectra are presented in Figs. 12 and 13. These examples are for 1-GeV protons on C and Ca. The experimental data for C are fairly well represented by the calculation except at 17.2° where the calculated spectrum is somewhat higher than experiment and peaks toward higher energies. The calculated spectra for Ca are higher than experiment for all three angles. This is due in part to the fact that the elastic cross sections used are somewhat too large at this energy. That is, the elastic cross section is taken to be the difference between the total cross section and the cross section for producing one pion. However, at this energy there is some double pion production which is largest for p-n collisions. If double pion production had been included, the p-n elastic cross section would be reduced by ~20%.[25] However, this is still not

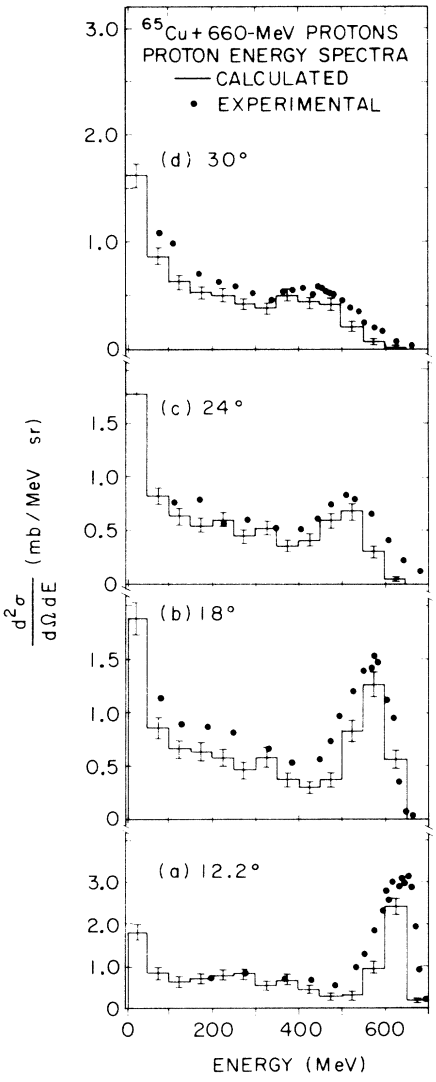

FIG. 11. Same as Fig. 10 but for Cu.

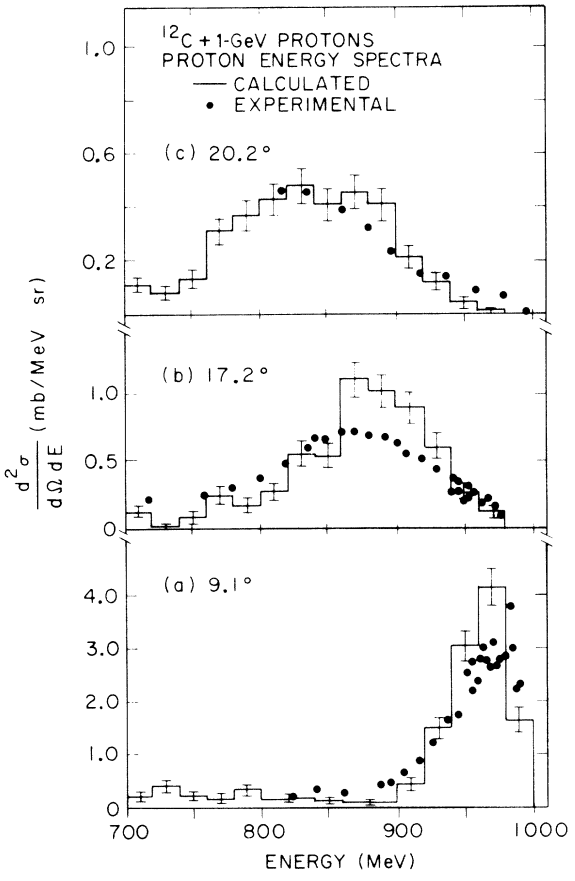

FIG. 12. Energy spectra of inelastic protons from the interaction of 1-GeV protons with C. The spectra are given at 9.1°, 17.2°, and 20°. The experimental points are taken from Ref. 24.

enough to account for the observed discrepancies.

Bertini[3] has also compared his results to this set of data. His spectra for both C and Ca are in somewhat better agreement with experiment than those predicted by the present model. However, his spectra for Ca are also larger than experiment.

C. Spallation yields

Calculated spallation yields depend not only on the particular intranuclear cascade model used but also on the manner in which the evaporation calculations are performed. Hence, they do not provide as direct a test of the intranuclear cascade model as those properties that were considered previously (i.e., pion yields and secondary particle spectra). In the present instance the evaporation calculations were done with a code described by Dostrovsky *et al.*[26]

In Table III calculated and experimental results[27-29] for the spallation of Al by 0.6- and 1-GeV protons are presented. The calculated results agree fairly well with experiment, except perhaps for the yields of the last three nuclei (i.e., ^{17}N, ^{13}N, and ^{11}C).

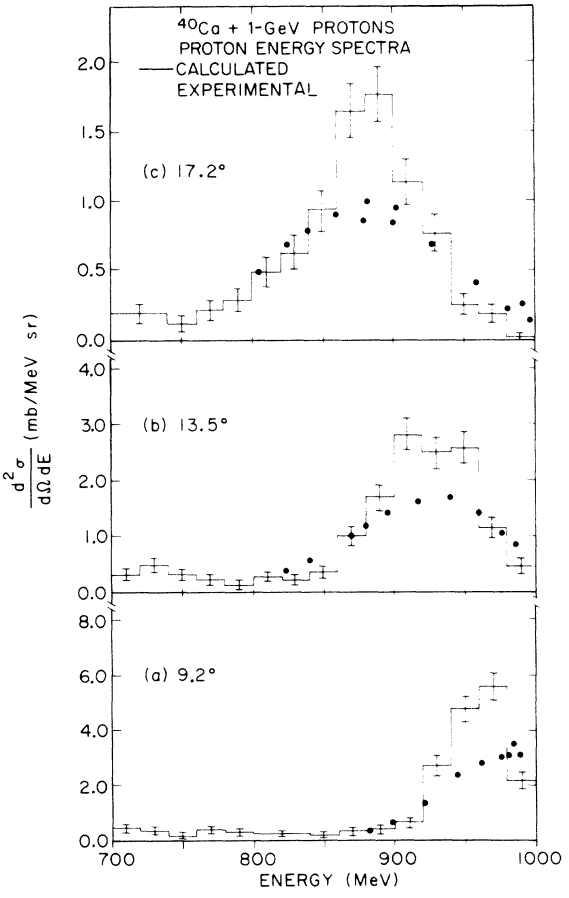

FIG. 13. Same as Fig. 12 but for Ca at 9.2°, 13.5°, and 17.2°.

TABLE III. Spallation cross sections for protons on ^{27}Al at 0.6 and 1 GeV. All cross sections are in mb.

Nuclide	Exp.	Calc.	Exp.	Calc.
^{24}Na [a]	10.8 ± 0.7	11.6 ± 1.5	10.5 ± 0.7	15.2 ± 1.8
^{22}Na [b]	19.2 ± 2.3	18.5 ± 1.9	16.7 ± 2.0	17.6 ± 1.9
^{21}Na + ^{21}Ne [c]	20.0 ± 3.0	19.5 ± 2.0		18.6 ± 2.0
^{22}Ne [c]	11.0 ± 2.0	5.1 ± 1.0		4.1 ± 0.9
^{20}Ne + ^{20}F [a]	20.0 ± 3.0	18.2 ± 1.9		16.7 ± 1.8
^{18}F [a]	7.9 ± 0.5	5.4 ± 1.0	8.0 ± 0.5	5.7 ± 1.1
^{15}O [c]	6.6 ± 2.0	3.6 ± 0.9	~6	3.5 ± 0.8
^{17}N [c]		0.14 ± 0.17	0.70	0.10 ± 0.14
^{13}N [c]	~1.3	3.7 ± 0.9	1.4 ± 0.1	4.3 ± 0.9
^{11}C [c]	~3	1.3 ± 0.5	4.3 ± 0.2	1.4 ± 0.5

[a] The adopted beam monitor cross sections of Cumming (Ref. 27).

[b] The experimental data of Friedlander *et al.* (Ref. 28) adjusted to the ^{24}Na cross sections of Cumming (Ref. 27).

[c] From the compilation of Silberberg and Tsao (Ref. 29). "Approximate" signs indicate interpolated values.

Further comparisons are presented in Table IV for the spallation of Cu by 590-MeV protons.[30] These results are representative of other comparisons that have been made with the model at this energy. The largest discrepancies occur for experimental cross sections which are ~1 mb or less. Typically, one can expect that ~80% or more of the calculated cross sections will differ from the experimental cross sections by a factor of 2 or less provided the experimental cross sections are greater than ~1 mb.

TABLE IV. Calculated and experimental (Ref. 30) spallation yields for the interaction of 590-MeV protons with Cu. All cross sections are in mb.

Nuclide	Experimental	Calculated
^{64}Cu	15.3 ± 7.0	15.6 ± 2.1
^{56}Ni	0.12 ± 0.03	0.37 ± 0.32
^{57}Ni	1.11 ± 0.09	2.0 ± 0.8
^{55}Co	1.75 ± 0.25	2.3 ± 0.8
^{56}Co	10.4 ± 1.2	14.3 ± 2.0
^{57}Co	29.3 ± 2.3	24.7 ± 2.7
^{58}Co	29.4 ± 2.4	15.5 ± 2.1
^{60}Co	12.8 ± 2.9	9.8 ± 1.7
^{52}Fe	0.26 ± 0.02	0.80 ± 0.50
^{59}Fe	1.86 ± 0.62	2.3 ± 0.8
^{52}Mn	9.2 ± 1.4	19.4 ± 2.3
^{54}Mn	21.7 ± 0.5	17.9 ± 2.3
^{48}Cr	0.37 ± 0.13	1.0 ± 0.5
^{51}Cr	26.9 ± 0.8	24.4 ± 2.6
^{48}V	10.3 ± 1.6	15.0 ± 2.1
^{46}Sc	4.94 ± 0.14	7.2 ± 1.4
^{47}Sc	2.17 ± 0.47	3.6 ± 1.0
^{48}Sc	0.49 ± 0.04	1.7 ± 0.7
^{42}K	1.53 ± 0.06	3.5 ± 1.0
^{43}K	0.57 ± 0.17	1.4 ± 0.6

IV. SUMMARY AND CONCLUSIONS

An intranuclear cascade model has been developed which considers the production and subsequent interactions of (3, 3) isobars produced in low-energy elastic pion-nucleon interactions and inelastic nucleon-nucleon and pion-nucleon interactions. From comparisons with experimental data that were made, it appears that the model gives a fair to excellent description of pion production in complex nuclei. The model also gives a reasonable description of the emission of high-energy nucleons in high-energy reactions, as well as the yields of radiochemical products produced in such reactions. Hence, the model should prove useful in designing and analyzing experiments done at Clinton P. Anderson Meson Physics Facility (LAMPF) and elsewhere.

ACKNOWLEDGMENTS

Helpful discussions with many colleagues, in particular with Dr. W. Rubinson, Dr. J. M. Miller, Dr. Z. Fraenkel, and Dr. G. Friedlander, are gratefully acknowledged. The author would also like to thank Mrs. M. Kinney for her assistance in the data reduction.

---

†Work supported by the U.S. Atomic Energy Commission.

*Present address: University of California, Los Alamos Scientific Laboratory, Los Alamos, New Mexico 87544.

[1]G. D. Harp, K. Chen, G. Friedlander, Z. Fraenkel, and J. M. Miller, Phys. Rev. C 8, 581 (1973).
[2]H. W. Bertini, Phys. Rev. 131, 1801 (1963).
[3]H. W. Bertini, Phys. Rev. 188, 1711 (1969); Phys. Rev. C 6, 631 (1972).
[4]N. Metropolis *et al.*, Phys. Rev. 110, 204 (1958).
[5]V. Barashenkov *et al.*, Acta Phys. Pol. 36, 457 (1969).
[6]V. Barashenkov and M. Maltsev, Z. Phys. 9, 549 (1961).
[7]D. Bugg *et al.*, Phys. Rev. 146, 980 (1966).
[8]K. Chen *et al.*, Phys. Rev. 166, 949 (1968).
[9]V. Barashenkov, V. M. Maltsev, I. Patera, and V. D. Toneev, Fortschr. Phys. 14, 357 (1966).
[10]J. Rushbrooke *et al.*, Nuovo Cimento 33, 1509 (1964).
[11]D. C. Brunt, M. J. Clayton, and B. A. Westwood, Phys. Rev. 187, 1856 (1969).
[12]A. Shapira *et al.*, Phys. Rev. Lett. 21, 1835 (1966).
[13]A. Dunaitsev *et al.*, Zh. Eksp. Teor. Fiz. 38, 747 (1960) [trans.: Sov. Phys.—JETP 11, 540 (1960)].
[14]Y. Bayukov, M. S. Kozodayev, Y. Prokoshkin, and A. A. Tyapkin, Nucl. Phys. 4, 61 (1957).
[15]T. Clements and L. Winsberg, UCRL Report No. UCRL-9043, 1960 (unpublished).
[16]G. Giacomelli *et al.*, Cern Report No. CERN/HERA 69-1, 1969 (unpublished).
[17]S. Lindenbaum and R. Sternheimer, Phys. Rev. 105, 1874 (1957); 109, 1723 (1958); 123, 333 (1961).
[18]E. Ferrari and F. Selleri, Nuovo Cimento Suppl. 24, 453 (1962).
[19]V. Suslenko and V. Kochkin, JINR Report No. P2-5572, Dubna, 1970 (unpublished).
[20]D. Bugg *et al.*, Phys. Rev. 133, B1017 (1964).
[21]D. R. F. Cochran *et al.*, Phys. Rev. D 6, 3085 (1972).
[22]A. Dunaitsev and Y. Prokoshkin, Nucl. Phys. 56, 300 (1964).
[23]L. Azhgirey *et al.*, Nucl. Phys. 13, 258 (1959).
[24]D. M. Corley *et al.*, Nucl. Phys. A184, 437 (1972).
[25]O. Benary *et al.*, UCRL Report No. UCRL-20000NN, 1970 (unpublished).
[26]I. Dostrovsky *et al.*, Phys. Rev. 116, 683 (1959).
[27]J. Cumming, Annu. Rev. Nucl. Sci. 13, 261 (1968).
[28]G. Friedlander *et al.*, Phys. Rev. 99, 261 (1955).
[29]R. Silberberg and C. Tsao, Astrophys. J. Suppl. 25, 315 (1973).
[30]C. Orth and H. O'Brien, Los Alamos Scientific Laboratories, private communication.